Geofísica Internacional (2026) **65-2**: 1- 11

Delineation of Sulfide Mineralization Zone Based on Geomagnetic and Induced Polarization (IP) Methods in Sangon-II, Kokap, Kulonprogo Districts, Yogyakarta

Y. Yatini[1], M Faizal Zakaria[1*] and Imam Suyanto[2]

Abstract

We used geomagnetic and 2D induced polarization (IP) methods to identify potential gold mineralization zones in the Sangon-II Kolonprogo area, Yogyakarta. Historical geological data indicate that gold mineralization is associated with quartz veins. Magnetic field measurements at 200 points and 8 IP lines were taken in the study area. The results of the Reduction to Pole (RTP) analysis of magnetic data and IP inversion modeling show how the mineralized areas are distributed. Low magnetic anomaly values (<500 nT), medium (500-1000 nT), and high values (>1000 nT) are interpreted as high, medium, and low alteration zones, respectively. By combining resistivity and chargeability values, the IP inversion results show the zoning of mineralized areas in the Sangon-II area. Low resistivity (<50 Ωm) to medium (50-300 Ωm) and high chargeability (>30ms) are zones of saturated water layers, soil on the surface of the weathering of igneous rocks. Resistivity (50-300 Ωm) and medium chargeability (10-30 ms) are alteration zones of silica-clay, argillic, and propylitic. Medium resistivity (50-300) Ωm and high chargeability (>30 ms) are sulfide mineralization zones. High resistivity (> 300 Ωm) and low chargeability (<10 ms) are unaltered volcanic rocks, andesite-rhyodacite, igneous rock, Nanggulan Formation. While resistivity (> 300 Ωm) and high chargeability (> 30 ms) are zones of igneous rock with high metal content as veins. The results of magnetic and IP analysis indicate the presence of a fault with the direction of N350E. This fault controls the alteration process and sulfide mineralization in the Sangon-II area. The distribution of mineralization areas is in the east, extending to the south, around the fault. The results of 3D modeling show that this area is quite promising.

Key words: Geomagnetic method, Induced Polarization, resistivity, chargeability, sulfides mineralization.

Resumen

Utilizamos métodos geomagnéticos y de polarización inducida (PI) 2D para identificar zonas de mineralización aurífera potencial en el área de Sangon-II Kolonprogo, Yogyakarta. Los datos geológicos históricos indican que la mineralización aurífera está asociada a vetas de cuarzo. Se tomaron mediciones del campo magnético en 200 puntos y 8 líneas de PI en el área de estudio. Los resultados del análisis de Reducción al Polo (RTP) de los datos magnéticos y el modelado de inversión de PI muestran la distribución de las áreas mineralizadas. Los valores bajos de anomalía magnética (<500 nT), medios (500-1000 nT) y altos (>1000 nT) se interpretan como zonas de alteración alta, media y baja, respectivamente. Al combinar los valores de resistividad y cargabilidad, los resultados de inversión de PI muestran la zonificación de las áreas mineralizadas en el área de Sangon-II. Baja resistividad (<50 Ωm) a media (50-300 Ωm) y alta cargabilidad (>30 ms) son zonas de capas de agua saturada, suelo en la superficie de la meteorización de rocas ígneas. Resistividad (50-300 Ωm) y cargabilidad media (10-30 ms) son zonas de alteración de sílice-arcilla, argílico y propilítico. Resistividad media (50-300) Ωm y alta cargabilidad (>30 ms) son zonas de mineralización de sulfuros. Alta resistividad (> 300 Ωm) y baja cargabilidad (<10 ms) son rocas volcánicas inalteradas, andesita-riodacita, roca ígnea, Formación Nanggulan. Mientras que resistividad (> 300 Ωm) y alta cargabilidad (> 30 ms) son zonas de roca ígnea con alto contenido de metal como vetas. Los resultados del análisis magnético y de polarización inducida (IP) indican la presencia de una falla con dirección N350E. Esta falla controla el proceso de alteración y la mineralización de sulfuros en el área Sangon-II. La distribución de las áreas de mineralización se encuentra al este, extendiéndose hacia el sur, alrededor de la falla. Los resultados del modelado 3D muestran que esta área es bastante prometedora.

Palabras clave: Método geomagnético, polarización inducida, resistividad, cargabilidad, mineralización de sulfuros.

Received: August 20, 2025; Accepted: January 4, 2026; Published on-line: April 1, 2026.

Editorial responsibility: Dr. Joel Rosales Rodríguez

* Corresponding author: Muhammad Faizal Zakaria, mfaizal@upnyk.ac.id

[1] Geophysics Engineering, Universitas Pembangunan Nasional Veteran Yogyakarta, SWK (104) North Ring Road Street Condong Catur 55283, Yogyakarta, Indonesia.

[2] Geophysics, Physic Department, Universitas Gadjah Mada, Yogyakarta, Indonesia.

Y. Yatini, M. Faizal Zakaria, Imam Suyanto

https://doi.org/10.22201/igeof.2954436xe.2026.65.2.1911

1. Introduction

The existence of mineral ore in Indonesia, especially on Java Island, is mostly formed by the magmatism process (hydrothermal). The mineral ore deposit in Indonesia is commonly placed in a sedimentation zone of low sulfidation epithermal. One of the distribution areas of the sedimentation zone for this type of gold is in Central Java (Hedenquist *et al.*, 2012; Sillitoe, 2000). Specifically, the area is in Kokap District, Kulonprogo, Special Region of Yogyakarta.

For a long time, Kokap District has been known as a community mining area. The exploration and exploitation by the local miners have been done in a simple way. It is done by looking for the quartz vein outcrops, which are considered to be associated with the surface gold, and then searching for the quartz vein's continuation. In exploitation, the locals dig with simple tools such as a hoe and a crowbar. The direction of the excavation was only based on an estimate, so the quartz vein was only discovered for several meters.

The gold mineral in this area results from hydrothermal deposition associated with intrusive rock such as Andesite, which comes from the Late Oligocene and is then deposited in rock fractures around it. Control of structures and lithology are dominated by intrusive and volcanic rocks crossed by sinistral strike-slip fault and normal fault. The deformation resulted in a fracture filled by hydrothermal fluid during the low-sulfidation epithermal mineralization process. The result of petrography analysis and atomic absorption spectrophotometry show that this area is part of hydrothermal system, which is dominated by alteration with a propylitic type. The gold grade (Au) found in this research is 1,274 ppm in the quartz vein (Pramumijoyo *et al.*, 2017; Purnamawati & Tapilatu, 2012).

The active tectonic and volcanic setting of epithermal systems increases the probability that will be covered by post-mineralization eruptive or sedimentary material (Locke *et al.*, 1999). Consequently, geophysical techniques can be particularly valuable in identifying subsurface alteration zones in the epithermal environment (Allis, 1990; Hedenquist *et al.*, 2000; Irvine & Smith, 1990). Geophysical techniques for mineral exploration are quite conventional, especially for metallic and non-metallic ores (Doyle, 1990; Yusefi *et al.*, 2017). Applying different geophysical techniques in mineral exploration has yielded mixed results, as it depends on the contrast in the physical properties of the target zones and host rocks (Camarero & Moreira, 2017; Lenhare & Moreira, 2020). Geoelectrical methods, i.e., direct current (DC) resistivity and Induced Polarization (IP), have been demonstrated to be a useful and effective tool in the exploration of mineral resources (metallic and non-metallic)(Bahri *et al.*, 2016; Mashhadi & Ramazi, 2018; Zhang *et al.*, 2019). This method can delineate different types of mineralization according to their types (Evrard *et al.*, 2018). Especially the IP method is widely used for mineral exploration because it is the only geophysical technique that can discriminate conductive or semiconductive minerals disseminated in a high electrical resistivity background (host rock) (Lévy *et al.*, 2019; Yatini *et al.*, 2019) and map changes in chargeability. IP is particularly effective at picking disseminated concentrations of conducting ore minerals. Identifying such sulfides is a significant pointer for gold occurrence as sulfide minerals such as pyrite and chalcopyrite are usually associated with economic gold occurrences.

This study aims to determine the existence of a sulfide mineralization area in Sangon-II, Kokap District, Kulonprogo, by combining the geomagnetic method and IP. The structure determination was developed, and the mineralization area was controlled using these methods. The interpretation of IP data determines the distribution of the mineralization area. The mineralization area and the genetic process image of the forming of Sangon-II were obtained by correlating the result of geomagnetic method modeling and IP with previous geology data. The magnetic measuring point location and IP data line are on the outside of the alteration area, which was made by (Pramumijoyo *et al.*, 2017) to expand the prospect area.

2. Geology Setting and Mineralization of The Research Area

According to (Raharjo *et al.*, 1995), the stratigraphy of the Kulonprogo Mountain Zone consists of several rock units: Quaternary volcanic rocks, alluvial deposits, an intrusion. These stratigraphic units are arranged from the oldest to the youngest as follows: Nanggulan Formation, Kebobutak Formation, Sentolo Formation, alluvial deposits, and Quaternary volcanic rocks.

According to Pramumijoyo *et al.*, (2017) The research area can be divided into two geomorphic units, namely intrusion dome and faulted hill, with the former unit named based on its tight, relatively rounded, and isolated contour patterns. (Pramumijoyo *et al.*, 2017). There are six rock units in the research area (Figure 1), they are including quartz wacke, intrusive andesite 1, intrusive andesite 2, diatreme breccia, intrusive andesite 3, and intrusive dacitic andesite. The quartz wacke is assumed to be a part of Axinea Beds in the Nanggulan Formation. It is composed of quartz and lithic wacke with a lamination structure with an N 112.5°E 55° trend.

The deposit formed in the hydrothermal location around the surface is called an epithermal deposit. This deposit has low temperature and pressure and usually can be found in the volcanic rocks. Epithermal mineral deposits are classified into two types: (1) low sulfidation, or adularia–sericite, and (2) high sulfidation or acid–sulfate (Hedenquist *et al.*, 2012; Purnamawati

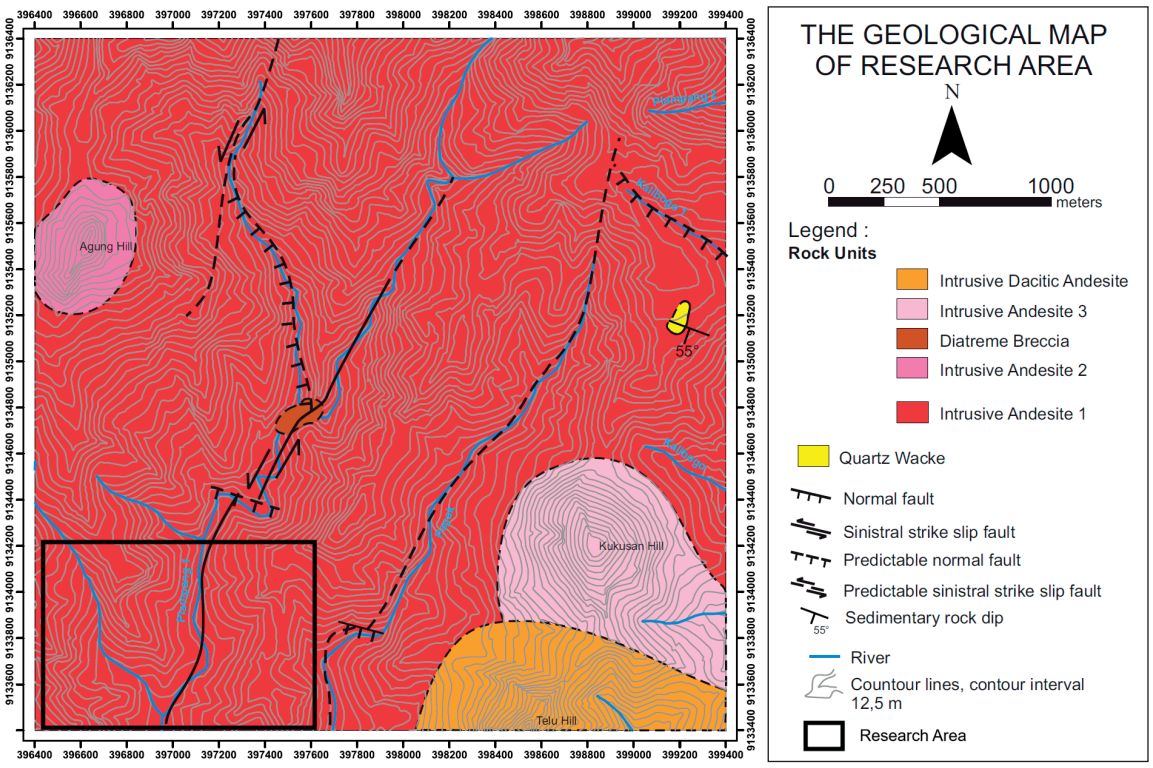


Figure 1. Local geological maps of Sangon-II and the surrounding area in Kokap District, the black box is the location of the research area (a modification from Pramumijoyo *et al.*, 2017).

& Tapilatu, 2012). The main differences between high and low sulfide epithermal are the chemical control and the type of fluids, which play a role in it. In high sulfide, the fluid that plays the role is sulfuric acid and is dominated by magmatic fluid. As for low sulfide, sulfuric acid and meteoric fluid plays a role.

High-sulfidation deposits commonly contain quartz, kaolinite, dickite, pyrophyllite, diaspore, and alunite. The alteration minerals indicate that these deposits formed from oxidized, acidic fluids; they commonly form above subvolcanic magma chambers (Arribas Jr, 1995). The common minerals found in the low-sulfide epithermal deposit type are pyrite, galena, sphalerite, chalcopyrite, silver, and gold. The other characteristic is the existence of sphalerite and arsenopyrite, which are commonly found in low-sulfide deposits. Those two minerals are rarely seen in the high-sulfide type. Gold and copper, such as enargite and luzonite, are commonly found in high-sulfide types. The source rocks in precious metal deposits with low sulfide are alkali andesite, rhyolite, dacite, and other alkali rocks. The deposit formation is dominated by quartz veins that fill the open space and are disseminated, commonly consisting of breccia veins.

The gold deposit in Sangon-II, Kokap District, is a low-sulfide type (Pramumijoyo *et al.*, 2017). The gold mineralization spread unevenly association between quartz veins, which consist of sulfide. The relation of sulfur and metal, found in this world in low to high grades and dimensions, is sometimes associated with phyllic-argillic altered clay. The spread of it is being controlled by fractured sections that formed stockwork veins. The quartz veins in the size 1-50 cm formed a mineralization line which commonly went in the direction N60˚E-N110˚E with a 70˚ to 80˚ slope. In some locations, the gold mineralization consists of thin quartz veins (1-50mm) that form stockwork veinlets in altered rock (Figure 2). Gold and silver are distributed randomly in quartz veins with grades 1 to 13.8 ppm Au and 5.4 to 63.2 ppm Ag (Handyarso & Kadir, 2017). In other places, the grade of Cu, Zn, Pb, Ag, and As grades up to 5171 ppm, 8995 ppm, 6398 ppm, 34.1 ppm, and 1010.5 ppm (Pramumijoyo *et al.*, 2017).

3. Methods

Identification of gold in quartz veins is carried out by applying the Geomagnetic and Induced Polarization (IP) method. The research location is in Sangon-II, Kalirejo, Kokap District, Kulonprogo. The geographical position is 7°50'54.78"S and 110° 3'44.69"E. The geomagnetic method is expected to obtain an accurate image of the structure. This geological structure controls the mineralization process. In addition, geomagnetic methods can be applied to determine the area's mineralization

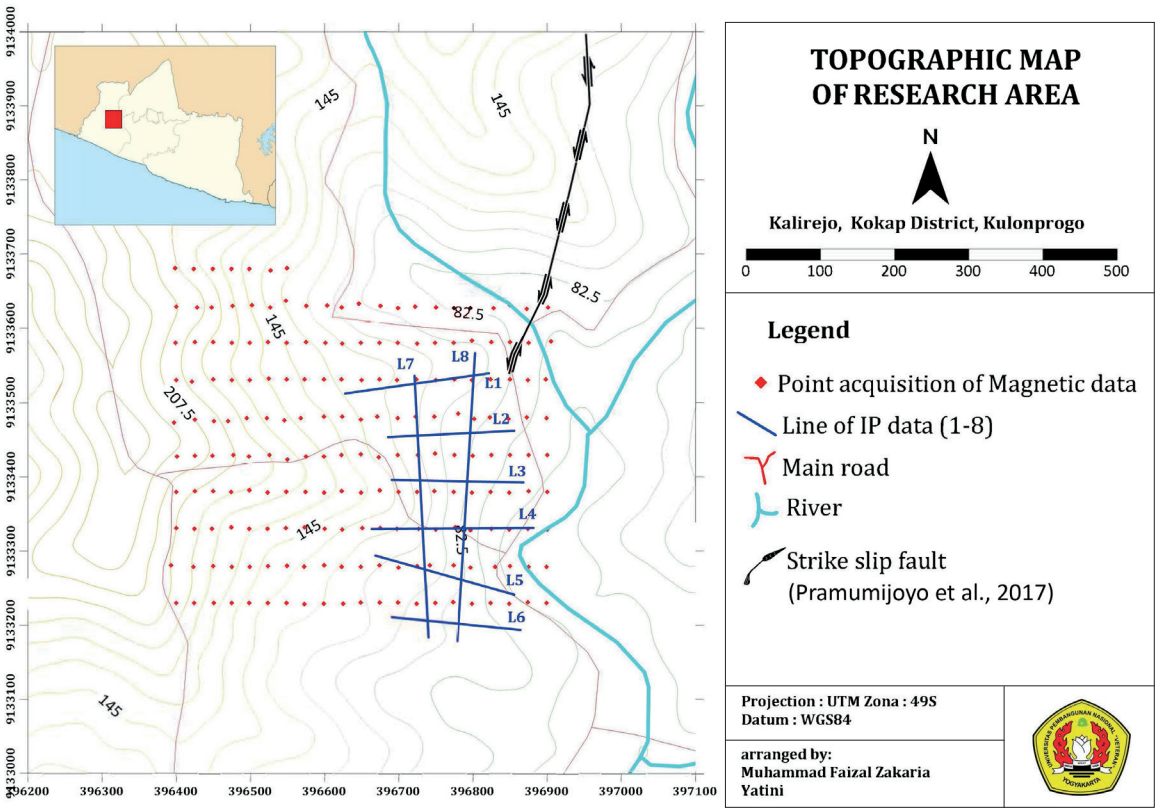


Figure 2. The survey design of Geomagnetic and IP data in Sangon-II, Kokap District, Kulonprogo. The red points show magnetic measurement points as many as 200, and the 8 lines of IP lines are presented in blue points.

type (Ercan *et al.*, 2014; Rabeh, 2009). Sulfide ore minerals can be distinguished from their magnetic properties because metallic minerals under normal conditions will have a high magnetic response (susceptibility) compared to non-metallic minerals. The IP method is applied to identify metal mineral content in the research area, based on the distribution of resistivity and chargeability values (Yatini *et al.*, 2019).

3.1 Geomagnetic

The geomagnetic method is one of the geophysical methods that utilizes the Earth's magnetic field which is caused by variations in the distribution of magnetized rocks below the surface. This method is based on the differences in the magnetization level of a rock induced by the earth's magnetic field. This happens as a result of differences in the rock's magnetic nature. This method is usually used to solve the problem of the crude oil exploration (Burazer *et al.*, 2001; Tong *et al.*, 2006), geothermal studies (Mohammadzadeh Moghaddam *et al.*, 2016; Zakaria, 2018), mineral rocks exploration (Ercan *et al.*, 2014; Rabeh, 2009), and applied to the prospecting research for archaeological objects (Boschi, 2012; Sarlak & Aghajani, 2017; Utama *et al.*, 2024).

The first stage in processing the geomagnetic data is quality control, which has the purpose of removing the noise from the magnetic observation result. In the next step, diurnal and IGRF were applied to eliminate the effects of external magnetic field and earth's main magnetic field. The measured magnetic field is reduced by diurnal variation and from the IGRF is obtaining an anomaly of the magnetic field for each measuring point. The IGRF values used in this study came from the National Oceanic and Atmospheric Administration (NOAA) website.

Geomagnetic data taken at Sangon-II at as many as 200 points formed a grid distributed in 10 lines. Each line is 50 meters apart, while the distance between points is 25 meters (Figure 2). The survey design of magnetic data points and IP paths is plotted on the alteration map (Pramumijoyo *et al.*, 2017). Geomagnetic method measurements use two sets of Geometrics G-856 type PPMs, which have an accuracy of 0.1 nT.

3.2 The induced polarization (IP)

The induced polarization (IP) method is based on a current-stimulated electrical phenomenon observed as a delayed voltage response in earth materials. The IP effect is observed as a

residual voltage decay after the current flow is interrupted (time domain IP) or as a frequency-dependent resistivity (frequency domain). In the time domain, the voltage decay is recorded during a time interval Δt = t2-t1 (ms) after the current flow is interrupted. The calculated parameter is the chargeability, given by

$$m = \frac{1}{V_0}\int_{t1}^{t2} V_t\,(t)dt \quad (1)$$

The first step in interpreting data in electrical tomography is to construct a pseudosection. This is obtained (Figure 3) by plotting the values of the apparent resistivity measured at the centre of the array and at a depth dependent on the spacing between the electrodes. The data were inverted by the Res2Dinv software using the Least Squares Inversion (Yatini, 2019).

The subsurface geology can probably have a form of beddings with different resistivity. The resistivity measurements made on the surface show a result called apparent resistivity (Yatini *et al.*, 2019). The measurement are done by injecting the current through current electrodes (C_1C_2) on the ground surface and measuring the potential in potential electrodes (P_1P_2). Dipole-dipole configuration is used by IP data acquisition (Figure 3). Dipole-dipole configuration of current electrodes (C_1C_2) and potential electrodes (P_1P_2), a is spacing and n = 1-6. The relationship of apparent resistivity and injected current (I), potential (ΔV), and configuration factor (K) is shown in equation (2).

$$\rho = \frac{\Delta V}{I}\,K \quad (2)$$

The geometry factor for the dipole-dipole electrodes arrangement is written in equation (3). In which a is the spacing of the electrodes and n = 1-8 or more.

$$K = \pi an(n+1)(n+2) \quad (3)$$

There are eight lines with varying lengths, six lines near-parallel, and there are two intersecting lines. IP data retrieval using Syscal Junior Type-586 IRIS IP-Meter Equipment. The IP-Meter type has a max output current of 1200 mA, a max power of 100W, and a cycle current of 0.5, 1, and 2 seconds. The integration time can be set to 500 ms. 1000 ms, and 2000 ms (Yatini, 2019). In this research, the integration time setting is 1000 ms. The dipole-dipole configuration is used for mapping, with a spacing of 10 and 20 meters and a value of n=1-8. There are eight lines with varying lengths from 210 meters to 400 meters. Several lines use 10-meter spacing and n=1-6, and 20-meter spacing with n=1-8. There are six tracks in the direction of N90°E and two in the direction of N180°E. The design of the Geomagnetic survey and IP lines is shown in Figure 3.

4. Results And Discussion

4.1 Magnetic Field Anomaly

The result of the magnetic field measurement in Sangon-II shows anomalies varying from 50 nT to 2600 nT. The Reduce to Pole (RTP) magnetic field anomaly is shown in Figure 4. Magnetic field anomaly response is strongly influenced by mineral composition of the rocks and geological processes in the research area.

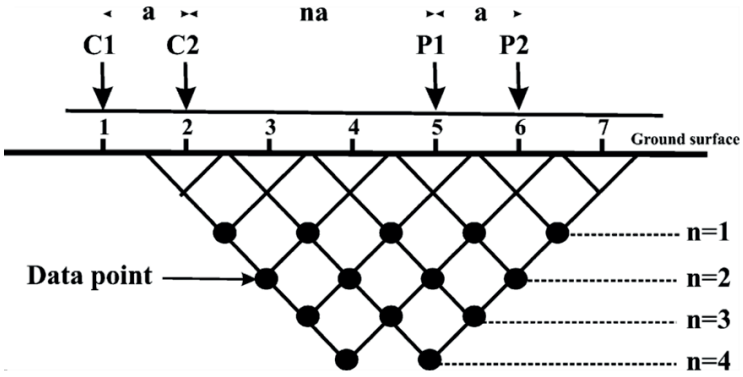


Figure 3. Configuration of the four-electrode DC dipole–dipole array used for resistivity profiling in this study. C_1 and C_2 are the current electrodes; P_1 and P_2 are the potential electrodes, while a is the spacing betwßeen electrodes used for each measurement and n is the expansion factor (integer values 1–8). The separation between dipoles is always a multiple (n) of a. Numbers 1–7 are the electrode (current and potential) station positions in meters(Adepelumi *et al.*, 2006)

The results of field observation found quartz veins in rock outcrops (Figure 1). Quartz vein samples were found to contain metal sulfide minerals. The measurement results of the magnetic method can show the distribution of quartz veins that contain metal sulfide minerals by looking at the distribution of anomaly field values in the area. Quartz veins are a type of metamorphic rock that is formed as a result of the intrusion of igneous rock that penetrates sedimentary rock. Then hydrothermal flow occurs, which will increase the temperature and pressure in the rock, resulting in mineralization (Sillitoe, 2000). Intrusive rock (igneous rock) has a very high susceptibility value, so igneous rock that intrudes sedimentary rock will have a higher magnetic susceptibility contrast than Sedimentary Rocks. Based on the formation process, the existence of quartz veins can be associated with the existence of intrusive rocks.

The high magnetic anomaly pattern distribution is in the northern part of the research area, extending to the center as shown in Figure 4. The high magnetic field anomaly value happens as the effect of rocks with high susceptibility surrounded by low susceptibility.

The reduced to pole magnetic field anomaly value was classified into three categories such as low values with total score less than 500 nT, medium (500-1000) nT high values with total score more than 1000 nT. Low field anomaly values (less than 500 nT) are interpreted as high mineralization zones. This zone is a zone that dominated by the presence of silicate mineralization and it is dominating the research area. Low magnetic field anomaly values were found in the E-S section (blue color) and slightly in the W-N section (index no 1 on the map), as shown in Figure 5. The high metal mineral content is most likely in the area. Metal mineral content such as enargite (CuAsS), chalcopyrite (CuFeS2), pyrite (FeS2), digenite (Cu9S5), gold (Au) and hematite (Fe2O3), were found in this zone. Gold and silver were found randomly distributed in quartz veins. In several places, Cu, Zn, Pb, Ag, and As grades up to 5171 ppm, 8995 ppm, 6398 ppm, 34.1 ppm, and 1010.5 ppm (Pramumijoyo *et al.*, 2017). The distribution of the existence of metallic minerals vertically and laterally is known from IP data, which is also measured in this area.

The contrast between the strong and moderate mineralization area is limited by something expected to be a fault. This fault is directed approximately in N350E. This fault continues the fault of (Pramumijoyo *et al.*, 2017) research area.

4.2 Induced Polarization Interpretation

IP targets likely represent sulfide-rich zones. According to Bahri *et al.*, (2016), if preexisting knowledge regarding the geological setting is available, resistivity and IP can help explore zone mineralization. The mineralization zone is delineated using the IP method by detecting the existence of sulfide minerals associated with Au metal. From the results of IP physical modeling, the resistivity inversion modeling is sensitive to recognizing the target's depth, position, and geometry (Apparao *et al.*, 2000; Sumner, 2012). However, it cannot be used to show a direct relationship with metal mineral content in the media below the surface. There is a positive correlation between the chargeability value, the existence of metallic minerals, and the content quantity. The higher the level (percentage of metal mineral content), the higher the chargeability value. In the IP time domain, the chargeability parameter determines the presence of metallic minerals below the surface. This principle is being used to interpret the results of the IP data inversion model in the Sangon-II area. The results of the inversion model using Res2DInv in all IP lines show the smallest resistivity value of 4 Ωm and the largest is 3900 Ωm. As in for the chargeability values, it varies from 1 ms to 95 ms. The resistivity and chargeability values in the research area are divided into 3 categories as shown in Table 2. The resistivity values are low (<50 Ωm), moderate in the range (50-300 Ωm) and high (>300 Ωm). The chargeability value is also categorized into 3 scales which are low, medium and high. The scale is low with a value (<10 ms), medium (10-30 ms), and high if the value is (< 30 ms). The classification of the scale of the resistivity and chargeability values of the research area in detail is in Table 1. The classification is necessary for interpretation by combining the resistivity and chargeability ranges with the results of surface observations and the compilation of alteration maps. The interpretation of the existing zones by combining resistivity and chargeability values are shown in detail in Table 2. The Sangon-II is divided into several types of zones and lithology:

1. Water layer zone. The resistivity value in this zone is low to moderate, while the chargeability value is low. The soil that is located on the surface is the result of weathering of volcanic rocks and igneous rocks. The porosity is quite high, resulting in the resistivity value strongly influenced by the weather when the survey was conducted. The resistivity value is low when the survey is conducted in the rainy and very high in the dry seasons. The chargeability value in this zone is low.
2. The alteration zones are developed (Pramumijoyo *et al.*, 2017) to be silica-clay (quartz-illite-kaolinite-kaolinite/smectite), argillic (smectite-illite/smectite), and propylitic (chlorite-calcite±epidote). The existence of silica minerals makes the resistivity value higher than the water layer zone. This zone has moderate resistivity and chargeability values. The existence of clay minerals due to alteration is indicated by moderate chargeability values with a maximum of 30 ms.
3. Magmatic differentiation in the study area allowed metals to be concentrated into a sulfide-rich phase as the magma cooled. Once sulfur saturation was reached, an immiscible

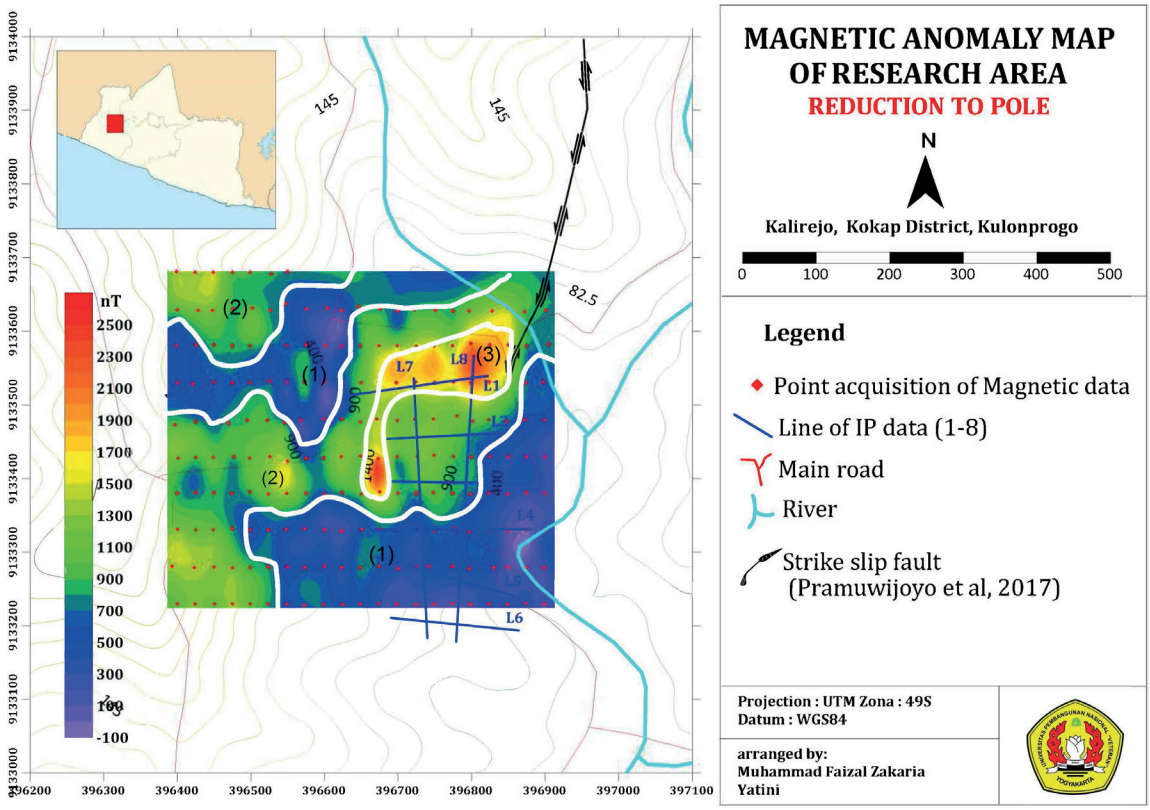


Figure 4. RTP anomaly magnetic field in Sangon-II, with contour interval as much as 50 nT. Three zones as a result of interpretation: (1) High alteration, (2) Medium alteration, and (3) Low alteration/igneous rock zone.

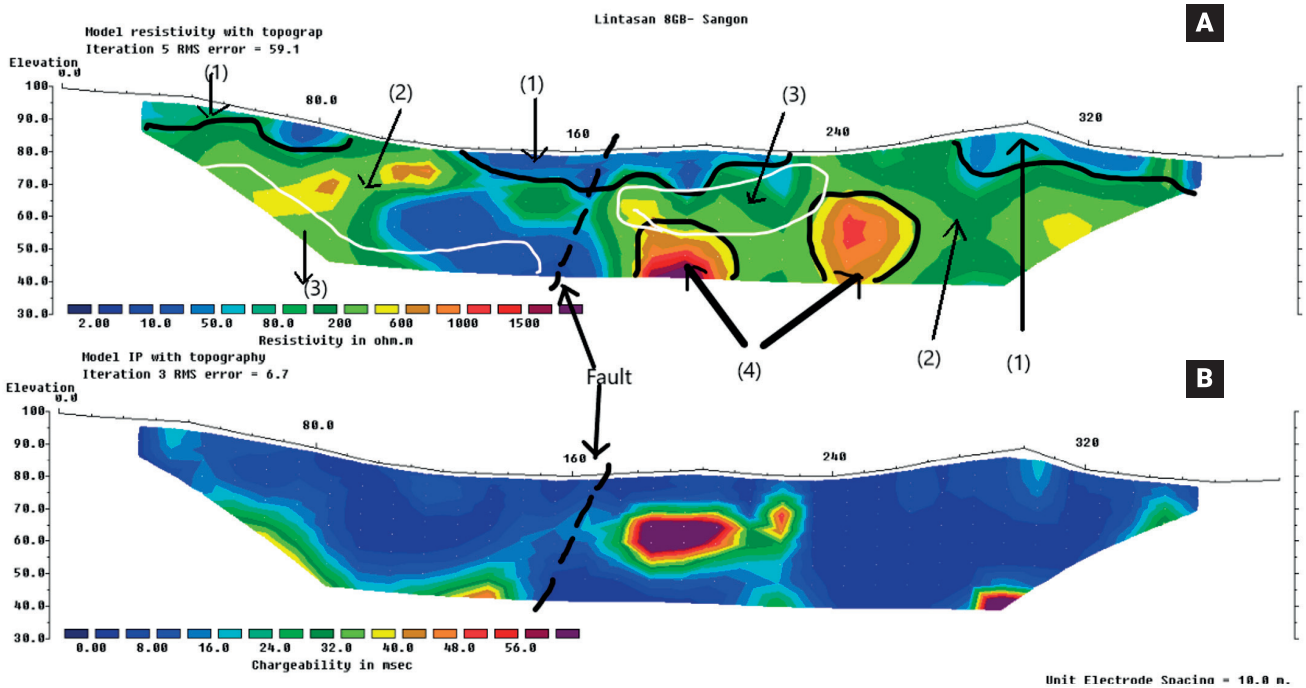


Figure 5. The interpretation of the mineralization zone of the IP modeling inversion results in lines L-8, incision A: resistivity and B: Chargeability. These lines have 4 zones: (1). Zone of saturated water layers, soil on the surface of the weathering of igneous rocks. (2). Alteration (3). Sulfide mineralization zone (4) Unaltered volcanic rocks, igneous rock.

Table 1. The classification of resistivity and chargeability in Sangon-II, Kokap, Kulonprogo

Scale	Resistivity-ρ(Ωm)	Chargeability-(ms)
Low	< 50	< 10
Medium	50-300	10-30
High	>300	>30

Table 2. Correlation of resistivity, chargeability value, and interpretation in Sangon-II, Kokap, Kulonprogo.

Resistivity-ρ(Ωm)	Chargeability (ms)	Interpretation
Low–medium	Low	Zone of saturated water layers, soil on the surface of the weathering of igneous rocks
Medium	Medium	The alteration zone silica-clay, argillic, and propylitic
Medium	High	Sulfide mineralization zona
High	Low	Unaltered volcanic rocks, Andesite-rhyodacite, Igneous Rock Nanggulan Formation
High	High	Igneous Rock Nanggulan Formation with high metal content

sulfide melt separated from the silicate melt and selectively incorporated metallic elements. The accumulation of these metallic sulfide minerals produced the geophysical characteristics observed in this zone, namely medium to high resistivity and high chargeability (>30 ms).

4. The units of andesitic and dacite igneous rocks that are part of the Nanggulan Formation. This igneous rock contains dominant silica quartz and other non-metallic minerals, so the resistivity value is high (>300 Ohm-m). Small metal mineral content is indicated by a low chargeability value (<10 ms).
5. Volcanic rock unit (igneous rock) has a fairly high metal mineral content. This zone is indicated by high resistivity and high chargeability values.

The results of the inversion model using Res2DINv for the L-8 path are shown in Figure 5. The fault zone is estimated to be at the 170th meters. The water-saturated zone, which is partly soil on the surface of the weathering of igneous rocks (1), is characterized by low to moderate resistivity values and low chargeability. This zone is spread over the 10th to 90th meters. Besides that, it is also found on the surface of the 120th to 230th meters, and at the southern end of L-8 from 270 to 360 meters. The depth of this zone is 9-10 meters in average.

The alteration zone (2) is characterized by moderate resistivity and chargeability values. This zone is evenly distributed from the end of the 10th meter to the end of the track at 360 meters. Some of it is exposed to 90 meters to 120 meters and 230 meters to 270 meters. The depth of this zone varies from 30 meters to 50 meters below the surface. On this L-8 trajectory, there are two zones of sulfide mineralization (3). This zone is characterized by medium resistivity and high chargeability values. The first zone is located at 45 to 150 meters with a depth of 25 meters to 30 meters from the surface. The second zone is located at 170 to 240 meters, at a depth of 7 meters to 15 meters. Unaltered volcanic rocks, Andesite-rhyodacite, or igneous rock (4), which are characterized by high resistivity values and low chargeability, are found at 190 meters and 240 meters at a depth of 25 meters and 15 meters.

The result interpretation of the other incision inversion was done using the same way and scheme with the L-8. At L-1 there is no soil zone on the surface and a little alteration zone, but there is no mineralization zone. The igneous rock unit is quite large, located at the end of the lines. The results of the interpretation of all trajectories were done in the same way, in order to obtain the distribution of mineralization areas towards vertical and lateral directions.

4.3 Distribution of Mineralization Area

Sangon-II, the research area, is located at the southwest end and has not been covered by the alteration(Pramumijoyo *et al.*, 2017). The value-added in this research is expanded the prospect area for sulfide mineralization in the Sangon area, Kokap District, Kulonprogo. The description of the quantitative distribution of the zones produced is based on a combination of IP, magnetic, and sample data on outcrops. The zones are classified based on the combination of resistivity and chargeability values, including (1) the Water layer or soil zone located on the surface of the soil, which is the result of weathering of volcanic and igneous rocks. (2) The alteration zones are developed to be

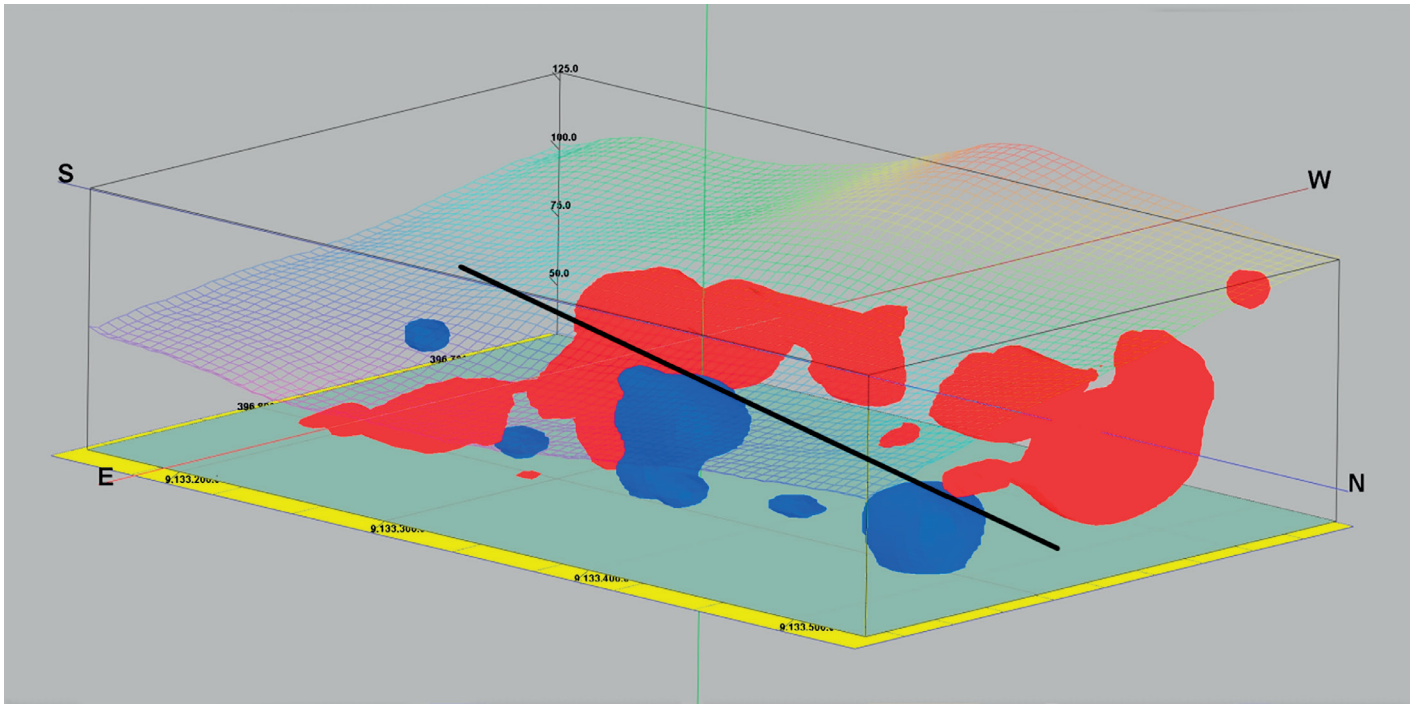


Figure 6. Distribution of sulfide mineralization zones (blue) from the results of IP data interpretation for the Sangon-II area. The black line shows the fault zone results from the inversion modeling of all IP data trajectories.

silica-clay (quartz-illite-kaolinite-kaolinite/smectite), argillic (smectite-illite/smectite), and propylitic (chlorite – calcite ± epidote). (3) Sulfide mineralization zone. (4). Zone of andesite or dacite igneous rocks and (5) Igneous rocks containing high levels of metal sulfide minerals.

The IP data interpretation shows that igneous rocks are spread almost everywhere in the research area, especially on the west. The depth varies from 10-14 meters. The sampling results in several outcrops show that the types of igneous rocks are andesite and dacite. This igneous rock is the source of alteration and caused sulfide mineralization in the Sangon-II area.

Some parts of igneous rock have high metal mineral content, indicated by high resistivity values and high chargeability. The existence of igneous rocks with such character was found on the L-2 trajectory to 110th at a depth of 15-20 meters from the surface. The trajectory is L-4 meters to 105 at a depth of 20-30 meters. The 270th L-7 in meter line at a depth of 30-40 meters, and the 230th L-8 meter track at a depth of 30-35 meters. The existence of high levels of metallic minerals in the igneous rocks of the Nanggulan Formation indicates that the potential for metallic minerals in the Sangon-II area is quite promising. Further research needs to be done by analyzing samples, in order to know the content of gold or other metals in igneous rocks with this characterization.

The alteration zone, which is alteration clay, argillic, and propylitic alteration, was found in the research area. Some of the alteration zones are exposed on the surface as shown in L-8, but most of them are below the surface. Most of this zone are on the above of the andesite and dacite igneous rocks, and some are between them. The sulfide mineralization zone was found in the alteration zone showed by the high chargeability values. A high chargeability value indicates a location that has a high metal mineral content (Yatini *et al.*, 2018). The overlay of the sulfide mineralization zone of Sangon-II is shown in Figure 6.

Inversion modeling on all IP trajectories in the Sangon-II area. It is expected to be a shear fault, directed to N350E. The existence of this fault is suspected to be a canal fault from the research of Pramumijoyo *et al.*, (2017) because the research area is outside it. Some of the sulfide mineralization zones are above the igneous rock zone. An illustration of the position of the sulfide mineralization zone against the igneous rock zone is shown in Figure 6. The distribution pattern of igneous rocks and metal sulphide mineralization zones around the fault shows that this fault structure controls the occurrence of hydrothermal alteration and mineralization in the Sangon-II area.

5. Conclusion

The magnetic measurement results show a fairly large range of magnetic anomaly values from 100 nT to 2600 nT, classified

into low, medium, and high. Three alterations were interpreted from magnetic anomalies, which were classified into high, medium, weak alteration, and igneous rock zones. The results of the magnetic analysis show an indication of a fault in the direction of N350E. The results of the IP method data inversion show that the resistivity range of the Sangon-II area is 5 to 3900 Ωm and chargeability is 1 to 95 ms. The range of resistivity and chargeability values are classified into low, medium, and high. Four zones are interpreted from IP data: saturated water layers, soil on the surface of the weathering of igneous rocks, Alteration, Sulfide mineralization zone, and Unaltered volcanic rocks igneous rocks. Igneous rocks are distributed almost evenly in the research area. The distribution of the mineralization area of the Sangon-II area extends from the east to the south around the fault. The 3D modeling results show that sulfide mineralization in Sangon-II area is quite prospective. The interpretation of IP data shows a fault with the direction of N350E, which is by the fault of the interpretation of geomagnetic data. Analysis of alteration zones, sulfide mineralization, and igneous rocks in the research area shows that this fault controls the alteration process and sulfide mineralization in the Sangon-II area.

6. Acknowledgment

The Institute of Research and Community Service of Universitas Pembangunan Nasional Veteran Yogyakarta funded this study on this occasion, the authors express deep gratitude and high appreciation to the institution for its support in running this research. The author also thanks the Sangon team, who helped retrieve IP and geomagnetic data.

7. References

Adepelumi, A. A., Yi, M.-J., Kim, J.-H., Ako, B. D., & Son, J. S. (2006). Integration of surface geophysical methods for fracture detection in crystalline bedrocks of southwestern Nigeria. Hydrogeology Journal, 14(7), 1284–1306. doi: **https://doi.org/10.1007/s10040-006-0051-2**

Allis, R. G. (1990). Geophysical anomalies over epithermal systems. Journal of Geochemical Exploration, 36(1–3), 339–374. doi: **https://doi.org/10.1016/0375-6742(90)90060-N**

Apparao, A., Srinivas, G. S., Sarma, V. S., Thomas, P. J., Joshi, M. S., & Prasad, P. R. (2000). Depth of detection of highly conducting and volume polarizable targets using induced polarization. Geophysical Prospecting, 48(5), 797–813. doi: **https://doi.org/10.1046/j.1365-2478.2000.00212.x**

Arribas Jr., A. (1995). Characteristics of high-sulfidation epithermal deposits, and their relation to magmatic fluid. Mineralogical Association of Canada Short Course, 23, 419–454.

Bahri, S., Zakaria, M. F., & Yatini, Y. (2016). Eksplorasi Mineral Menggunakan Metode Polarisasi Terinduksi di Daerah Kasihan, Kecamatan Tegalombo, Kabupaten Pacitan. [Bachelor's Thesis]. Universitas Islam Negeri Sunan Kalijaga.

Boschi, F. (2012). Magnetic prospecting for the archaeology of Classe (Ravenna). Archaeological Prospection, 19(3), 219–227. doi: **https://doi.org/10.1002/arp.1430**

Burazer, M., Grbović, M., & Žitko, V. (2001). Magnetic data processing for hydrocarbon exploration in the Pannonian Basin, Yugoslavia. Geophysics, 66(6), 1669–1679. doi: **https://doi.org/10.1190/1.1486769**

Camarero, P. L., & Moreira, C. A. (2017). Geophysical investigation of earth dam using the electrical tomography resistivity technique. REM-International Engineering Journal, 70(1), 47–52. doi: **https://doi.org/10.1590/0370-44672016700099**

Doyle, H. A. (1990). Geophysical exploration for gold; a review. Geophysics, 55(2), 134–146. doi: **https://doi.org/10.1190/1.1442820**

Ercan, Ö. A., Şeren, A., & Elmas, A. (2014). Gold and Silver Prospection Using Magnetic, Radiometry and Microgravity Methods in the Kışladağ Province of Western Turkey. Resource Geology, 64(1), 25–34. doi: **https://doi.org/10.1111/rge.12024**

Evrard, M., Dumont, G., Hermans, T., Chouteau, M., Francis, O., Pirard, E., & Nguyen, F. (2018). Geophysical Investigation of the Pb–Zn Deposit of Lontzen–Poppelsberg, Belgium. Minerals, 8(6), 233. doi: **https://doi.org/10.3390/min8060233**

Handyarso, A., & Kadir, W. G. A. (2017). Gravity Data Decomposition Based on Spectral Analysis and Halo Wavelet Transform, Case Study at Bird's Head Peninsula, West Papua. Journal of Engineering & Technological Sciences, 49(4), 423-437. doi: **https://doi.org/10.5614/j.eng.technol.sci.2017.49.4.1**

Hedenquist, J. W., Arribas, A., & Gonzalez-Urien, E. (2000). Exploration for epithermal gold deposits. In S. G. Hagemann & P. E. (Eds.), Brown, Gold in 2000 (pp. 245–277). Society of Economic Geologists. **https://doi.org/10.5382/Rev.13.07**

Hedenquist, J. W., Harris, M., & Camus, F. (2012). Geology and Genesis of Major Copper Deposits and Districts of the WorldA Tribute to Richard H. Sillitoe. Society of Economic Geologists. doi: **https://doi.org/10.5382/SP.16**

Irvine, R. J., & Smith, M. J. (1990). Geophysical exploration for epithermal gold deposits. Journal of Geochemical Exploration, 36(1–3), 375–412. doi: **https://doi.org/10.1016/0375-6742(90)90061-E**

Lenhare, B. D., & Moreira, C. A. (2020). Geophysical prospecting over a meta-ultramafic sequence with indicators of gold mineralization in Rio Grande do Sul State, Southernmost Brazil. Pure and Applied Geophysics, 177(11), 5367–5383. doi: **https://doi.org/10.1007/s00024-020-02559-0**

Lévy, L., Maurya, P. K., Byrdina, S., Vandemeulebrouck, J., Sigmundsson, F., Árnason, K., Ricci, T., Deldicque, D., Roger, M., & Gibert, B. (2019). Electrical resistivity tomography and time-domain induced polarization field investigations of geothermal areas at Krafla, Iceland: comparison to borehole and laboratory frequency-domain electrical observations. Geophysical Journal International, 218(3), 1469–1489. doi: **https://doi.org/10.1093/gji/ggz240**

Locke, C. A., Johnson, S. A., Cassidy, J., & Mauk, J. L. (1999). Geophysical exploration of the Puhipuhi epithermal area, Northland, New Zealand. Journal of Geochemical Exploration, 65(2), 91–109. doi: **https://doi.org/10.1016/S0375-6742(98)00067-3**

Mashhadi, S. R., & Ramazi, H. (2018). The application of resistivity and induced polarization methods in identification of skarn alteration haloes: A case study in the Qale-Alimoradkhan Area. Journal of Environmental and Engineering Geophysics, 23(3), 363–368. doi: **https://doi.org/10.2113/JEEG23.3.363**

Mohammadzadeh Moghaddam, M., Mirzaei, S., Nouraliee, J., & Porkhial, S. (2016). Integrated magnetic and gravity surveys for geothermal exploration in Central Iran. Arabian Journal of Geosciences, 9, 506. doi: **https://doi.org/10.1007/s12517-016-2539-y**

Pramumijoyo, P., Idrus, A., Warmada, I. W., & Yonezu, K. (2017). Geology, geochemistry and hydrothermal fluid characteristics of low sulfidation epithermal deposit in the Sangon Area, Kokap, Special Region of Yogyakarta. Journal of Applied Geology, 2(1), 48–58. doi: **https://doi.org/10.22146/jag.42442**

Purnamawati, D. I., & Tapilatu, S. R. (2012). Genesa Dan Kelimpahan Mineral Logam Emas, Dan Asosiasinya Berdasarkan Analisis Petrografi, Dan Atomic Absorbtion Spectrophotometry (Aas), Di Daerah Sangon, Kabupaten Kulonprogo, Propinsi Diy. Jurnal Teknologi, 5(2), 163–171. **https://ejournal.akprind.ac.id/index.php/jurtek/article/view/976**

Rabeh, T. (2009). Prospecting for the ferromagnetic mineral accumulations using the magnetic method at the Eastern Desert, Egypt. Journal of Geophysics and Engineering, 6(4), 401–411. doi: **https://doi.org/10.1088/1742-2132/6/4/008**

Raharjo, W., Sukandarrumidi, R. H. M. D., & Rosidi, H. M. D. (1995). Peta Geologi Lembar Yogyakarta, Jawa,[map] 1: 100.000. Bandung: Direktorat Geologi.

Sarlak, B., & Aghajani, H. (2017). Archaeological investigations at Tepe Hissar-Damghan using gravity and magnetics methods. Journal of Research on Archaeometry, 2(2), 19–34. doi: **https://doi.org/10.29252/jra.2.2.19**

Sillitoe, R. H. (2000). Styles of high-sulphidation gold, silver and copper mineralisation in porphyry and epithermal environments. Proceedings of the Australasian Institute of Mining and Metallurgy, 305(1), 19–34.

Sumner, J. S. (2012). Principles of induced polarization for geophysical exploration. Elsevier.

Tong, M., Li, L., Wang, W., & Jiang, Y. (2006). A time-domain induced-polarization method for estimating permeability in a shaly sand reservoir. Geophysical Prospecting, 54(5), 623–631. doi: **https://doi.org/10.1111/j.1365-2478.2006.00568.x**

Utama, B. S., Yatini, Y., Giamboro, W. S., & Hamdallah, H. (2024). Application of Geoelectric Method to Determine the Distribution of Liyangan Temple in Central Java. AMERTA, 42(2), 123–136. doi: **https://doi.org/10.55981/amt.2024.4932**

Yatini, Y. (2019). Influence of clay on time domain induced polarization, Indonesian Journal of Science and Technology, 3(1), 1-10. doi: **https://doi.org/10.17509/ijost.v3i1.10794**

Yatini, Y., Santoso, D., Laesanpura, A., & Sulistijo, B. (2018). Physical Modeling on Time Domain Induced Polarization (TDIP) Response of Metal Mineral Content. Indonesian Journal of Applied Physics, 8(2), 57–66.

Yatini, Y., Suyanto, I., & Puspaningrum, D. (2019). Application of polarization method (IP) to delineate the gold mineralization zones in Cihonje Areas, Banyumas Regency, Province of Central Java. IOP Conference Series: Materials Science and Engineering, 546(7), 072013. doi: **https://doi.org/10.1088/1757-899X/546/7/072013**

Yusefi, M. R., Hafizi, M. K., & Salari, B. (2017). Gold exploration using induced polarization and resistivity methods in Meyduk-Latala area. 79th EAGE Conference and Exhibition 2017, 2017(1), 1–3. doi: **https://doi.org/10.3997/2214-4609.201701546**

Zakaria, M. F. (2018). Identification of Heat Source and Alteration Zone of Parangwedang Geothermal System using Magnetic Method. EAGE-HAGI 1st Asia Pacific Meeting on Near Surface Geoscience and Engineering, 2018(1), 1–4. doi: **https://doi.org/10.3997/2214-4609.201800342**

Zhang, G., Lü, Q.-T., Lin, P.-R., & Zhang, G.-B. (2019). Electrode array and data density effects in 3D induced polarization tomography and applications for mineral exploration. Arabian Journal of Geosciences, 12, 1–17. doi: **https://doi.org/10.1007/s12517-019-4341-0**